Influence of Well Pattern on in situ Stress Filed of Shale Reservoir

Li Shuai[1,2(✉)], Chen Junbin[1,2], Li Yu[1,2], and Liu Jing[1,2]

[1] Shaanxi Key Laboratory of Well Stability and Fluid & Rock Mechanics in Oil and Gas Reservoirs, Xi'an Shiyou University, Xi'an 710065, Shaanxi, China
{lishuai_xsy, chenjbxu}@163.com
[2] College of Petroleum Engineering, Xi'an Shiyou University, Xi'an 710065, Shaanxi, China

Abstract. The form of well pattern is the key factor affecting the change of reservoir pore pressure. Due to the fluid–solid coupling effect of the reservoir, the distribution characteristics of the stress field in the reservoir under different well network forms have a significant difference. The study of the distribution of the stress field of the shale reservoir can provide the basis for the design of oil well fracturing, the stability evaluation of the well wall, and the adjustment of the development scheme et al. Based on the geostress model of Huang Rongzun, this paper takes the basic injection and production unit of well pattern as the research object, and explores the distribution characteristics of pore pressure and ground stress under different well network when the injection and production balance. The results show that: (1) in a short time, when the reservoir rock and fluid parameters are constant, the pore pressure is inversely proportional to the maximum principal stress and is directly proportional to the minimum principal stress; (2) under fixed pressure and production, the pore pressure, maximum principal stress, and minimum principal stress of 5-, 7-, 9-point well pattern changed rapidly in the near wellbore area 100–200 m and remained unchanged after 200 m. In 4-point well pattern, the relationship between stress and distance varies logarithmically. There are obvious differences between the three pressure variations and amplitude under different well pattern.

Keywords: Shale · Well pattern · Initial stress field · Stress distribution after production

J. Lin (ed.), *Proceedings of the International Field Exploration and Development Conference 2018*, Springer Series in Geomechanics and Geoengineering, https://doi.org/10.1007/978-981-13-7127-1_152

1 Introduction

The "shale gas revolution" in the USA has changed the world's energy structure. Shale as an unconventional reservoir has become a research hotspot. According to the China Institute of engineering, the Ministry of land and resources, China Petroleum and Natural Gas Group Corporation (China Petroleum), China Petrochemical Group Co., Ltd. (Sinopec) and other institutions, and China's shale gas resources have relatively good prospects for development [1–3]. At present, the shale development in China has basically completed the stage of resource assessment. Further understanding of the shale reservoir will be the key factor for shale gas development, and the analysis of the stress field of the reservoir is an important factor in understanding the shale reservoir environment. The analysis of the reservoir stress field is the key factor for the exploration and development of shale oil and gas resources [4–7]. The analysis of the reservoir stress field is very important for all aspects of exploration and development of shale oil and gas resources. During the exploration stage, the evolution of crustal stress controls the migration and accumulation of oil and gas; In the drilling stage, the distribution of in situ stress determines the wellbore stability and casing safety; In the design stage of the development plan, the stress field determines the choice of well pattern and production system; In the stage of reservoir reconstruction, the design of initial fracturing and refracturing is determined by the distribution of geostress field. A large number of scholars, such as, Yishan [8], Hong [9], Yan [10], Wangsheng [11], and the others all agree that the distribution of the stress field at each stage of the reservoir is of great significance to the development of the reservoir.

2 Common Ground Stress Models

There are many factors affecting the distribution of geostress field, and pore pressure is the most important factor. From the basic theory of fluid–solid coupling, it is known that when the pore pressure changes, the pressure of rock skeleton will change; in other words, the ground stress field will change. As for the reservoir fluid–solid coupling, a large number of previous studies have been done. These equations have a common characteristic that the calculation of the equations is large and the solution is complex and there are many required dynamic parameters needed, and the general practical application is more troublesome. Therefore, in order to facilitate the field application, a large number of simple mathematical models are generated [12–17].

(1) Mattews-Kelly

$$\sigma_{h2} = k_i\left(\sigma_v - p_p\right) + p_p \tag{1}$$

(2) Eaton

$$\sigma_{h2} = \frac{\mu}{1-\mu}(\sigma_v - p_p) + p_p \tag{2}$$

The above model considers that the pressure gradient of the overlying strata is independent of the depth and does not take into account the influence of the Biot coefficient, which is inconsistent with the actual situation; In addition, the stress coefficient K_i of the skeleton should be determined by fracturing data from adjacent wells, so the applicability of the model is not strong.

(3) Aliderson

$$\sigma_{h2} = \frac{\mu}{1-\mu}(\sigma_v - ap_p) + ap_p \tag{3}$$

The Anderson model has greatly improved the calculation of in situ stress. The introduction of Biot's coefficient has led to a further understanding of pore pressure.

(4) Newberry

$$\sigma_{h2} = \frac{\mu}{1-\mu}(\sigma_v - ap_p) + p_p \tag{4}$$

Newberry improved the Anderson model through the low-permeability formation with microfracture.

(5) Thiercelin

$$\begin{aligned} \sigma_H &= \frac{\mu}{1-\mu}(\sigma_v - ap_p) + \frac{E}{1-\mu^2}\varepsilon_H + \frac{E\mu}{1-\mu^2}\varepsilon_h \\ \sigma_h &= \frac{\mu}{1-\mu}(\sigma_v - ap_p) + \frac{E}{1-\mu^2}\varepsilon_h + \frac{E\mu}{1-\mu^2}\varepsilon_H \end{aligned} \tag{5}$$

The above model is suitable for areas with relatively severe structure. For areas with relatively gentle structure, a model established by Professor Huang Rongzun in the study of the fracturing pressure of the formation can be used.

(6) Huang Rongzun

$$\begin{aligned} \sigma_H &= \left(\frac{\mu}{1-\mu} + A\right)(\sigma_V - aP_p) + aP_p \\ \sigma_h &= \left(\frac{\mu}{1-\mu} + B\right)(\sigma_V - aP_p) + aP_p \end{aligned} \tag{6}$$

This model is the most widely used model at present. The model is not only simple, but also relatively accurate.

It can be seen from model (7) that the Huang Rongzun model has good applicability in constructing gentle areas. The model not only takes into account the force difference between the vertical and horizontal direction of the reservoir but also considers the difference of the mechanical properties of the rock in a horizontal direction. Because of considering many factors, it has been widely used. In this paper, Huang Rong Lu model is used to explore the influence of pore pressure on the in situ stress field.

3 The Common Seepage Model of Reservoir

There are mainly three kinds of seepage models in reservoirs: one-dimensional seepage, plane radial flow, and spherical flow. And radial flow is the most common model. Fluid seepage can be divided into stable and unstable percolation. In a relatively short time, the fluid is considered to be steady seepage, but the unstable percolation in the general reservoir. In order to simplify the discussion and illustrate the problem, the following assumptions are made:

(1) The reservoir is infinite, homogeneous, equal thickness, and incompressible;
(2) Fluid is incompressible, and the flow parameters remain unchanged during the flow process;
(3) Fluid seepage follows Darcy's law;
(4) The reservoir is completely filled with oil and gas, and the injection drive is rigid drive;
(5) There is no physical and chemical reaction between reservoir rock and fluid;

For the radial unsteady seepage flow in a plane, the pore pressure expression is:

$$p(r,t) = p_i + \frac{\mu q}{4\pi kh} Ei\left(-\frac{r^2}{4\eta t}\right) \tag{7}$$

It is known from the percolation mechanics that if n wells are produced at the same time in the large wireless formation, the output of each well is Q_i, and the time of production is τ_i, and the position of the well is (X_i, Y_i), of which, i =1, 2,… n, the pressure drop at any point M (x, y) at any time is shown in Eq. (8):

$$\Delta p = -\frac{u}{4\pi kh} \sum_{i=1}^{n} \pm q_i Ei\left[-\frac{\left[(x-x_i)^2 + (y-y_i)^2\right]}{4\eta(t-\tau_i)}\right] \tag{8}$$

In Eq. (8), take the positive number ahead of the oil well Q_i and take the minus sign for the injection well Q_i.

When there is only one well in the plane, the rule of pore pressure and ground stress with time and distance can be obtained by using the following parameter Table 1.

Table 1. Basic parameters

Modulus of elasticity (E) (GPa)	10
Stress coefficient of geological structure (A)	0.80
Bottom-hole pressure of the production well (Pw) (MPa) Bottom-hole pressure of the production well (Pw) (MPa)	10
Fluid viscosity (mpa.s)	0.75
Well radius (rw) (m)	0.10
Boundary radius of reservoir (re) (m)	1000
Overlying rock stress (σv) (MPa)	20
Pressure coefficient (η) (m^2/s)	2
Poisson ratio (v)	0.25
Stress coefficient of geological structure (B)	0.20
daily oil production (Water injection) (q) (m^3/d)	100
reservoir permeability (k) (μm^2)	0.50
formation thickness H (m)	5
Supply boundary pressure (Pe) (MPa)	20
Effective stress coefficient (a)	0.80
distance between the oil well and the origin	50

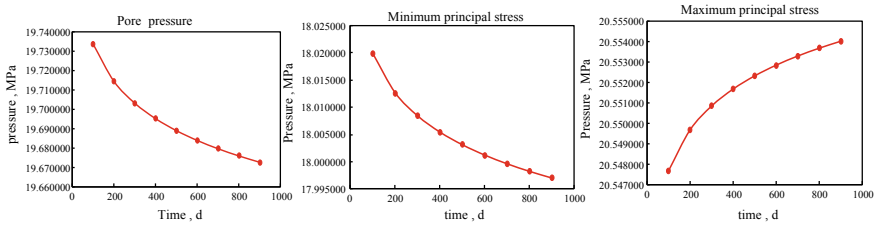

Fig. 1. Relationship between stress and time of radial unsteady seepage in the reservoirs

For unsteady seepage, the pore pressure is not only related to the time, but also related to the distance, so the control variable is used, when r = 50 m, the stress changes with time as shown in Fig. 1.

As can be seen from Fig. 1, for the research point at r = 50 m, the pore pressure and the minimum principal stress gradually decrease with time, the decreasing amplitude decreases and the maximum principal stress increases with time, but the increase is gradually reduced.

When the production time is t = 1000 d, the variation of stress with time is shown in Fig. 2.

As can be seen from Fig. 2, when the time is t = 1000 d, the pore pressure and the minimum principal stress increase with the increase of distance, but the amplitude of the increase gradually decreases, and the maximum principal stress decreases with the increase of distance, and the decrease is also decreasing.

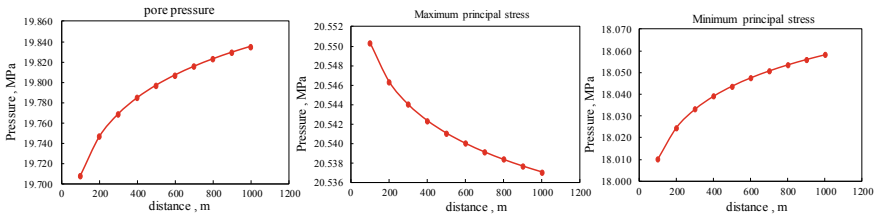

Fig. 2. Relationship between stress and distance of radial unsteady seepage in reservoir

4 The Distribution Characteristics of Ground Stress Under the Common Well Network

For complex well network, For example, the common 5-point well pattern, 7-point well pattern, and 9-point well pattern can be taken as the research object of the basic injection production unit. If the interference between the injection and production units is ignored, a well pattern can be regarded as duplication of several injection production units. The pressure drop at any point in the formation can be regarded as the algebraic sum of the pressure drop produced by each injection production unit at this point. In order to facilitate the study, it is assumed that each injection production unit has reached the injection and production balance, that is, the energy lost at any point in the formation due to the recovery of the well can be supplemented in time by the increased energy of the injection well, that is, the pressure drop of any point in the stratum is not changed with time, only a function of distance [18].

(1) 5-point water injection development well network

The injection and production unit of the 5-point injection well network is shown in Fig. 3, consisting of one injection wells and four production wells [7]. The coordinates of injection and production wells are respectively as follows: (0, 0), (a, a), (a, $-a$), ($-a$, a), ($-a$, $-a$).

At any point, the pore pressure is

$$p(x,t) = p_i - \frac{qu}{4\pi kh}R$$

$$R = 4\ln\frac{(x^2+y^2)}{(x-a)^2+(y-a)^2} - \ln\left[(x-a)^2+(y+a)^2\right] - \ln\left[(x+a)^2+(y-a)^2\right] - \ln\left[(x+a)^2+(y+a)^2\right] - 2.886 \tag{9}$$

As the injection production unit is completely symmetrical about the X-axis and the Y-axis, it is only necessary to calculate the special point at the 100–900 m axis of the X-axis, bringing the data in Table 1 into formula (10) and the Huang rongzun model, we can get the pressure distribution in this kind of well pattern.

As can be seen from Fig. 4, the pressure of the pore pressure on the X-axis is reduced between 100–900 m, but the maximum decrease is between the 100 and

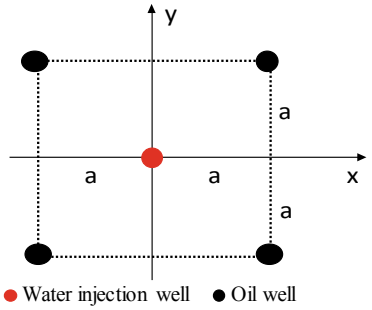

Fig. 3. Injection and production unit of 5-point water injection well network

200 m. After the 200 m, the pore pressure is most stable, the formation pressure decreases at a minimum rate, and after a certain distance, the pressure remains unchanged. The maximum principal stress increases rapidly between 100 and 200 m, and then tends to be stable after 200 m.

(2) 9-point water injection development well network

The injection production unit of the 9-point water injection development well network is shown in Fig. 5. From the chart, it can be seen that the injection production unit of the well pattern is composed of one water injection wells and eight production wells.

In the coordinate axis shown in Fig. 5, the coordinates of the water injection well are (0, 0), the coordinates of the oil wells are (a, 0), (a, a), (a, $-a$), (0, a), (0, $-a$), ($-a$, a), ($-a$, $-a$), and ($-a$, 0). At any point, the pore pressure is:

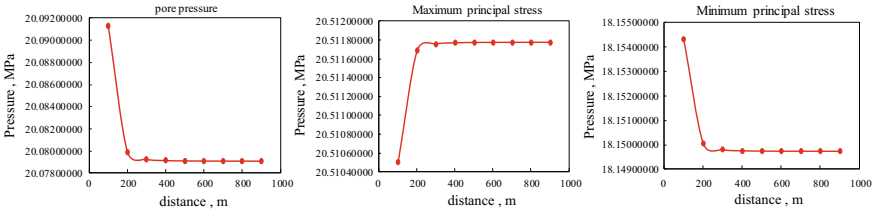

Fig. 4. Relationship between the stress and the distance of the 5-point method reservoir

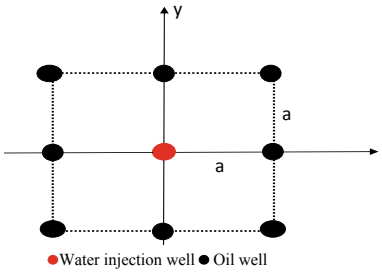

Fig. 5. Injection and production unit of 9-point water injection well network

$$
\begin{aligned}
p(x,t) &= p_i - \frac{qu}{4\pi kh}R \\
R &= 8\ln\left(x^2+y^2\right) - \ln\left[(x-a)^2+y^2\right] \\
&\quad - \ln\left[(x-a)^2+(y-a)^2\right] - \ln\left[(x-a)^2+(y+a)^2\right] \\
&\quad - \ln\left[x^2+(y-a)^2\right] - \ln\left[x^2+(y+a)^2\right] - \ln\left[(x+a)^2+(y-a)^2\right] \\
&\quad - \ln\left[(x+a)^2+(y+a)^2\right] - \ln\left[(x+a)^2+y^2\right] - 5.1948
\end{aligned}
\tag{10}
$$

Bringing the data in Table 1 into formula (10) and the Huang Rongzun model, we can get the pressure distribution in this kind of well pattern. As the injection production unit is completely symmetrical about the *X*-axis and the *Y*-axis, it is only necessary to calculate the special location on the *X*-axis.

It can be seen from Fig. 6 that the variation rule of pore pressure, maximum principal stress, and minimum principal stress of the 9-point well pattern is the same as that of the 5-point method.

(3) 7-point water injection development well network

The injection and production units of the 7-point water injection development well network are shown in Fig. 7:

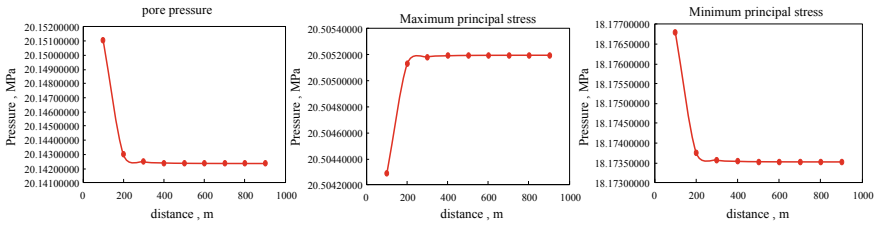

Fig. 6. Relationship between the stress and the distance of the 9-point method reservoir

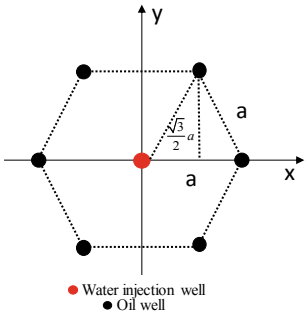

Fig. 7. Injection and production unit of 7-point water injection well network

As can be seen from Fig. 7, the injection production unit of the 7-point injection well is composed of one injection well and six wells. In the coordinate axis shown in the figure, the coordinates of the injection wells are (0, 0), the coordinates of the oil wells are $(a, 0)$, $(-a, 0)$, $\left(a/2, -\frac{\sqrt{3}}{2}a\right)$, $\left(a/2, -\frac{\sqrt{3}}{2}a\right)$, $\left(-a/2, \frac{\sqrt{3}}{2}a\right)$, $\left(-a/2, -\frac{\sqrt{3}}{2}a\right)$.

At any point, the pore pressure is:

$$
\begin{aligned}
p(x,t) &= p_i - \frac{qu}{4\pi kh}R \\
R &= 6\ln\left(x^2+y^2\right) - \ln\left[\left[(x-a)^2+y^2\right]\right. \\
&\quad \left.\left[(x+a)^2+y^2\right]\right] - \ln\left[\begin{array}{r}(x-a/2)^2 \\ +\left(y-\sqrt{3}a/2\right)^2\end{array}\right] \\
&\quad - \ln\left[\begin{array}{r}(x+a/2)^2 \\ +\left(y-\sqrt{3}a/2\right)^2\end{array}\right] - \ln\left[\begin{array}{r}(x+a/2)^2+ \\ \left(y+\sqrt{3}a/2\right)^2\end{array}\right] \\
&\quad - \ln\left[\begin{array}{r}(x-a/2)^2+ \\ \left(y+\sqrt{3}a/2\right)^2\end{array}\right] - 4.0404
\end{aligned}
\tag{11}
$$

Bringing the data in Table 1 into the formula (11) and Huang Rongzun model, we can get the pressure distribution in this kind of well pattern. The research point is elected on the *X*-axis, and the relationship between the stress and distance is shown in Fig. 8.

The research point is selected on the *Y*-axis, and the relationship between the stress and distance is shown in Fig. 9.

From Figs. 8 and 9, it can be seen that the pore pressure, the maximum principal stress, and the minimum principal stress on the *Y*-axis are the same as that of the 5-point method and the 9-point method on the 7-point well network, but on the *X*-axis, the law of change is just the opposite.

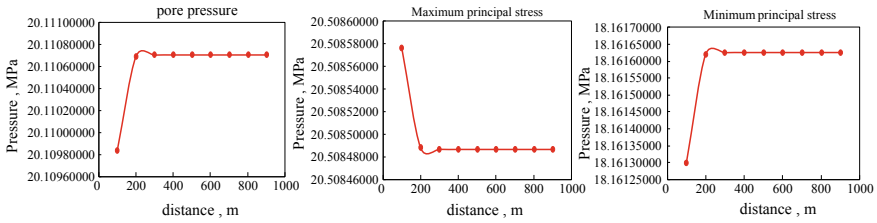

Fig. 8. Relationship between the stress and the distance of the 7-point method reservoir

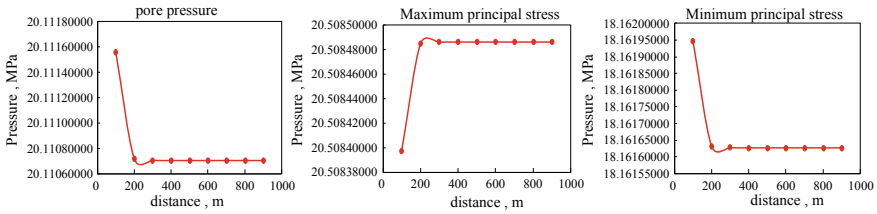

Fig. 9. Relationship between the stress and the distance of the 7-point method reservoir

(4) 4-point water injection development well network

The injection and production unit of the 4-point water injection development well network is shown in Fig. 10:

As can be seen from Fig. 10, the 4-point injection production unit consists of one water injection well and three production wells. In the coordinate system as shown in Fig. 10, the coordinates of water injection well is $\left(\sqrt{3}a/3, 0\right)$, and the coordinates of production wells are $(-a, 0)$, $(a, 0)$, and $\left(\sqrt{3}a, 0\right)$, at any point, the pore pressure is:

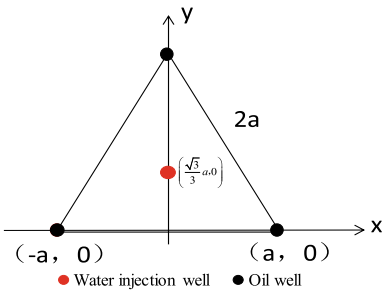

Fig. 10. Injection and production units of 4-point water injection well network

$$p(x,t) = p_i - \frac{q_1 u}{4\pi kh} R$$
$$R = \ln\left[\left(x - \sqrt{3}a/2\right)^2 + y^2\right] - \ln\left[(x-a)^2 + y^2\right] - \ln\left[(x+a)^2 + y^2\right] - \ln\left[\left(x - \sqrt{3}a\right)^2 + y^2\right] \quad (12)$$

Bringing the data in Table 3 into formula (12) and the Huang Rongzun model, the research point is selected on the *X*-axis, and the relationship between the stress and distance is shown in Fig. 11.

The research point is selected on the *Y*-axis, and the relationship between the stress and distance is shown in Fig. 12.

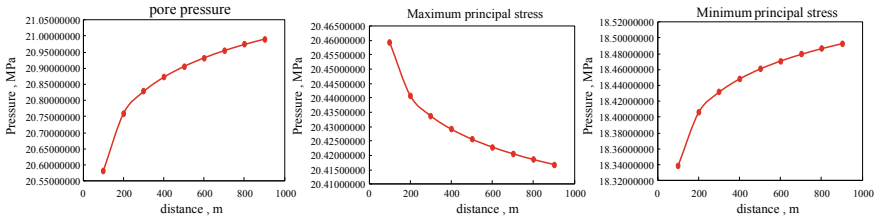

Fig. 11. Relationship between the stress and the distance of the 4-point method reservoir

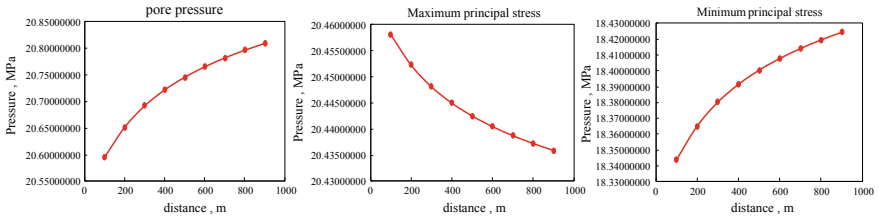

Fig. 12. Relationship between the stress and the distance of the 4-point method reservoir

As shown in Figs. 11 and 12, the variation laws of the research points on the *X*-axis and the *Y*-axis are basically the same. The pore pressure and the minimum principal stress increase with the increase of distance, but the amplitude of the increase is decreasing, and finally tends to be stable. The maximum principal stress decreases with the increase of distance, and the decrease is steadily decreasing and finally tends to be stable. The difference is that the research point of *X*-axis changes fast at 100–200 m, and the *Y*-axis changes slowly in 100–200 m.

5 Conclusion

(1) In a short period of time, the maximum principal stress of the reservoir is inversely proportional to the pore pressure, and the minimum principal stress of the reservoir is directly proportional to the pore pressure. The change of pore pressure is the main reason for the change of crustal stress.
(2) For a single well-exploited reservoir, when fluid flow is unstable percolation, at some point, the greater the distance between the research point and the wellbore, the greater the pressure is, but the increase range is decreasing. At a certain location, the pore pressure decreases with the increase of time, but the magnitude of reduction decreases.
(3) When the well pattern is different, the variation of pore pressure in the reservoir is also different. well pattern of the 5-point method and the 9-point method are completely symmetric, So the change law of pore pressure is the same. The basic injection and production unit of the 7-point well network is asymmetrical, and the variation rule of pore pressure is opposite between the line direction of production wells and the line direction of injection wells and production wells. In the 4-point method well network, the variation rule of pore pressure is same between the line direction of production wells and the line direction of injection wells and production wells, but the range of change is different, and along the line direction of production wells, pore pressure changes drastically in the near well area.

Acknowledgements. Thanks to **National Natural Science Foundation Project:** Study on brittle failure mechanism of shale reservoirs based on meso–macro mechanics (51674197) funded.

References

1. Wenzhi Z, Dazhong D, Jianzhong L, et al. The resource potential and future status in natural gas development of shale gas in China. Eng Sci. 2012;14(7):46–52.
2. Caineng Z, Dazhong D, Yuman W, et al. Shale gas in China: characteristics, challenges and prospects (I). Petrol Explor Dev. 2015;42(6):689–701.
3. Zhang J, Xu B, Nie H, et al. Exploration potential of shale gas resources in China. Nat Gas Indus. 2008;28(6):136–40.
4. Han Z. Research on mechanics mechanism in refracturing and its applications. Chin Univ Petrol. 2012.
5. Yanxiang Y. Application of stress information to improvement of well allocation. Petrol Explor Dev. 1997;24(4):80–2.
6. Yuntao W, Jianwen Y, Wensi C. Application of reservoir stress characteristics to low permeability oilfield development design. Petrol Geol & Oilfield Dev Daqing. 2005;24 (5):30–2.
7. Zekai Liu, Yaolin Chen, Ruzhong Tang. Application of in-situ stress technology in oil field development. Oil Gas Recovery Technol. 1994;1(1):48–56.
8. Yishan Lou. The application of geostress in the development of oil and gas field. Petrol Drilling Tech. 1997;3:58–9.

9. Liu Hong Hu, Yongquan Zhao Jinzhou, et al. Simulation study of induced stress field in refracturing gas well. Chin J Rock Mech Eng. 2004;23(23):4022.
10. Deng Y. Study on mechanical mechanism of refracturing forming new fractures. Southwest Petrol Univ. 2005.
11. Tian W. A study on the mechanism of refracturing. Chin Univ Petrol. 2008.
12. Liang T. Study of relation between in-situ stress and borehole stability. Chin Univ Geosci. 2012.
13. Jingen Deng, Zhengrong Chen, Yanan Geng, et al. Prediction model for in-situ formation stress in shale reservoirs. J Chin Univ Petrol (Ed Nat Sci). 2013;37(6):59–64.
14. Li Y. A study on the stress distribution of low permeability oilfield refracturing. Chin Univ Petrol (Beijing). 2012.
15. Hongkui Ge. Distribution of in-situ stresses in oilfield. Fault-Block Oil and Gas Field | Fault-Block Oil Gas Field. 1998;05(5):1–5.
16. Zhao JYF. The logging calculation and calibration methods for crustal stress. Sci Technol Eng. 2015;15(17):42–6.
17. Zhou X, Zhang L, Fan K. Measurement of the present earth stress of Ordos Basin and its applications in oil and gas exploitation. J Xian Shiyou Univ (Nat Sci Ed). 2009;24(3):7–12.
18. Wang B, Zhang S, Li L. The Well pattern optimization design methed based on the earth stress filed. 2007;26(3):55–59.